The 2nd Spitzer Conference: Infrared Diagnostics of Galaxy Evolution
ASP Conference Series, Vol. 381, ©2008
Ranga-Ram Chary, Harry I. Teplitz, Kartik Sheth, eds.

Ultradeep Spectroscopy with the *Spitzer*[1] IRS[2]

H. I. Teplitz,[3] V. Desai,[3] L. Armus,[3] R. Chary,[3] J. W. Colbert,[3] D. T. Frayer,[3] A. Pope,[5] A. Blain,[4] H. Spoon,[6] V. Charmandaris,[7] D. Scott[5] and S. Antonucci[8]

Abstract. Mid-IR spectroscopy has detected the signatures of star-formation (PAH emission) in high redshift ($z > 1$) ultra- and hyper-luminous infrared galaxies. However, the study of the dominant population of IR-luminous galaxies (10^{11} - 10^{12} Lsun at $1 < z < 3$), requires observation of sources a at the 0.1 mJy level. We present the deepest spectra taken to date in the Long-Low module of the the Infrared Spectrometer (IRS) on the *Spitzer Space Telescope*. We targeted two faint ($\sim$ 0.15 mJy) sources in the Southern GOODS field at $z =$ 1.09 and $z = 2.69$ as likely star-forming galaxies. Spectra of the lower redshift target were taken in 8-21 micron range (short-low first order and long-low second order), while the higher redshift target was observed from 21-37 microns (long-low first order). Observing times were 3 and 9 hours on-source for SL-1 and LL-2, respectively, and 12 hours for LL-1. We also present the spectra of two serendipitous sources. We detect strong PAH emission in four targets. We compare the spectra to those of local galaxies observed by the IRS. The $z =$ 1.09 source appears to be a typical, star-formation dominated LIRG, while the $z = 2.69$ source is a composite source with strong star formation and a prominent AGN. The AGN component dominates the IRAC colors of this source, obscuring the 1.6 μm "bump." Such sources would be excluded from IRAC surveys for starbursts which might then underestimate the star formation density.

1. Introduction

More than 70% of the stars at redshifts $z > 0.5$ were formed during an infrared luminous phase (Elbaz et al. 2002) in which galaxies were identifiable as LIRGs ($10^{11} < L_{IR} < 10^{12}$ $L_\odot$) or ULIRGs ($L_{IR} > 10^{12}$ $L_\odot$). These sources are responsible for the peak of the faint 24 micron number counts that was previ-

[1]Based on observations obtained with the *Spitzer Space Telescope*, which is operated by JPL, California Institute of Technology for the National Aeronautics and Space Administration

[2]The IRS is a collaborative venture between Cornell University and Ball Aerospace Corporation that was funded by NASA through JPL.

[3]Spitzer Science Center, MS 220-6, Caltech, Pasadena, CA 91125

[4]Astronomy Department, Caltech, Pasadena, CA 91125

[5]Dept of Physics & Astronomy, University of British Columbia, Vancouver, BC V6T1Z1, Canada

[6]Astronomy Department, Cornell University, Ithaca, NY 14853

[7]University of Crete, Dept. of Physics, GR-71003 Heraklion, Greece

[8]Department of Physics, UCSB, Santa Barbara, CA 93106

ously undetected by ISOCAM (Papovich et al. 2004; Marleau et al. 2004). In particular, LIRGs rather than ULIRGs dominate at $1 < z < 2$ (Lagache et al. 2004; Chary et al. 2004; Pérez-González et al. 2005). As much as 85% of this luminosity may be generated by star formation (Bell et al. 2005; Brand et al. 2006), although that fraction is uncertain.

High redshift IR luminous galaxies are easily detected by *Spitzer* imaging surveys (GOODS, SWIRE, COSMOS) but have been beyond the reach of large IRS spectroscopy programs of high redshift sources, which have mostly been limited to $f_{24} > 0.8$ mJy (Houck et al. 2005; Yan et al. 2005). While these programs sample the most extreme, hyperluminous ($> 10^{13}$ $L_\odot$) sources, they find a significant fraction of sources show evidence of strong star formation (Yan et al. 2005; Lutz et al. 2005).

In order to push the limits of the MIR spectroscopy of the *Spitzer Space Telescope* into realm of typical high redshift LIRGs and ULIRGs, we targeted two faint (0.15 mJy) galaxies at $z \geq 1$. The program was granted 32 hours of Director's discretionary time. In this paper, we present the results of those observations, demonstrating for the first time the capability of the Infrared Spectrograph (IRS Houck et al. 2004) to detect continuum emission at such faint flux levels. Throughout, we assume a Λ-dominated flat universe, with $H_0 = 70$ km s^{-1} Mpc^{-1}, $\Omega_\Lambda = 0.7, \Omega_m = 0.3$.

2. Observations

We select targets from the southern field of the Great Observatories Origins Deep Survey (GOODS). We choose two sources, one with an *Chandra* detection and one without. We constrain the X-ray source to have a ratio of X-ray to infrared luminosity that is consistent with many submillimeter galaxies (SMGs Alexander et al. 2005). We selected both sources in the UDF area, and avoided sources with highly compact morphologies. A final selection criterion was the redshift, which we selected to place the strongest PAH features in the center of one of the IRS slits. By selecting one source at $z \sim 1$ and one at $z \sim 2.5$, we were able to obtain spectra covering the 6.2, 7.7 and 8.6 μm PAH features in just one or two slits.

We selected a z=2.69 object with $f_{24} = 0.15$ mJy, Source 1, and a z=1.09 object with $f_{16} = 0.15$ mJy, Source 2. Given the experimental nature of the observations, we were able to choose observation dates which were favorable for including serendipitous sources in the slit. Two secondary objects are of particular interest, and these are indicated in the figure: (1) an X-ray source detected by *Chandra*, but lacking an optical redshift, referred to hereafter as Source 2-x; and (2) a source lacking optical redshift but selected to be at high redshift by the *BzK* selection technique (Daddi et al. 2005), referred to hereafter as Source 1-BzK.

For the z=1.09 target, we obtained observations in Long-Low second order spectrum (LL-2, $14-21$ μm) in *Staring Mode*. In this mode, the target is placed at two "nod" positions within the slit. At each nod position we took 70 spectra of 120 sec ramp duration. The total integration time was 9 hours. We also observed this target in the short-wavelength low-resolution slit, in the first order (SL-1), for three hours on source in *Staring Mode*.

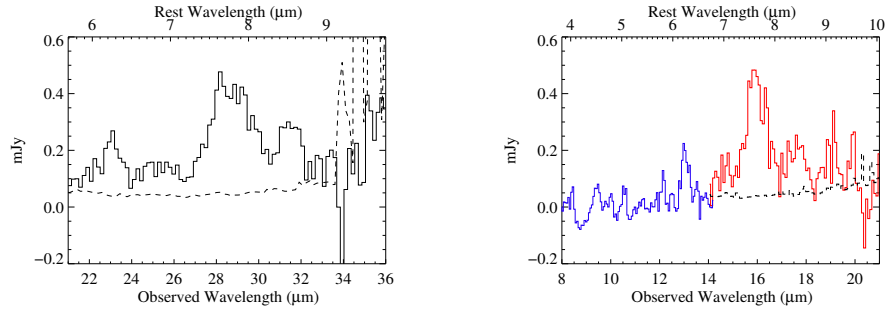

Figure 1. The spectra of the primary targets, Source 1 (right; LL-1) and Source 2 (left; SL-1, thin line; LL-2, thick line). The 1σ LL error arrays are shown (dashed lines).

For the higher redshift target, we used the Long-Low first order spectrum (LL-1, $21-37$ μm). These observations were obtained in *Mapping Mode*, wherein the target is placed at six positions along the slit. The observations were broken into three AORs of four hours each, with 20 spectra of 120 sec ramp duration at each of the six map positions, for a total on-source integration time of 12 hours.

All observations were scheduled immediately after the "skydark" calibrations in order to maximize the sensitivity by reducing the change of latent images from a preceding bright target.

3. Results

Figures 1 and 2 show the spectra of the primary and secondary targets. The continuum level is in good agreement with the estimate from the broad-band photometry at 16 and 24 μm. Broad emission features, identified as polycyclic aromatic hydrocarbon (PAH) emission, are detected at rest wavelengths of 6.2, 7.7, and 8.6 μm, along with the continuum at the blue end of LL-2 and LL-1.

The PAH features in Source 1-BzK confirm that it is at high redshift, $z = 2.55$. The other secondary source, Source 2-x, shows a single emission line

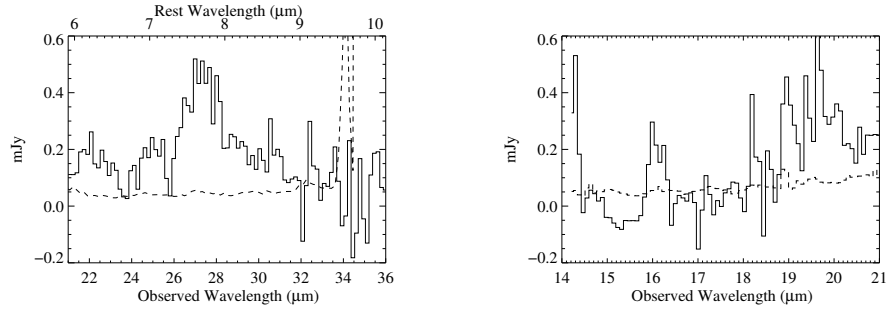

Figure 2. The spectra of the secondary targets, Source 1-BzK (right; LL-1) and Source 2-x (left; LL-2). The 1σ LL error arrays are shown (dashed lines).

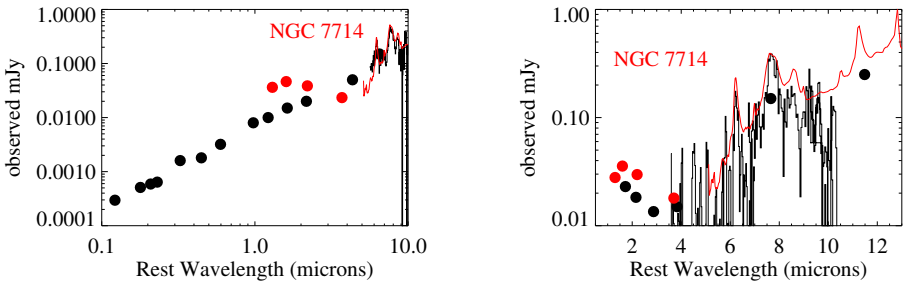

Figure 3. The spectra and photometry of the primary targets, Source 1 (right; LL-1) and Source 2 (left), compared to the SED of the local starburst NGC 7714 (red).

at$\sim$ 16 μm, and possibly enhanced emission at $\sim$ 19 μm. If the isolated line were identified with the 6.2 μm PAH feature, the object would be at $z \sim 1.5$.

The SNR at 16 μm in LL-2 and 24 μm in LL-1 is generally consistent with the predictions of *SPEC-PET* on the SSC website. The *SPEC-PET* predictions do not include noise introduced by the pipeline processing or spectral extraction. They also assume the spectra are smoothed to R=50, which we have not done. *SPEC-PET* predicts a 12 hour integration in LL-1 will yield a 3σ uncertainty of 0.12 mJy at 24 μm with R=50. Our measured 3σ uncertainty is $\sim$ 0.13 mJy. *SPEC-PET* predicts a 9 hour integration in LL-2 will yield a 3σ uncertainty of 0.08 mJy at 16 μm and R=50. Our measured uncertainty is $\sim$ 0.12 mJy. While both spectra have noise values close to the *SPEC-PET* prediction, the *Mapping Mode* observation gives noticeably better results.

4. Discussion

Both of the primary targets show strong PAH emission, indicative of star formation. Source 1-BzK also clearly shows PAH emission. If the single emission line in Source 2-x arises from PAH, then it may be a starburst as well. The comparison is similar for both Source 2 and Source 1-BzK. The equivalent width and the ratio of the 6.2 to 7.7 μm PAH equivalent widths of the PAH features in all three objects is similar to that of local starbursts. It is not surprising that that the BzK object or the $z = 1.09$ LIRG show prominent starburst indicators. However, one might have expected the $z = 2.69$ *Chandra* source to have a more featureless spectrum, perhaps dominated by strong silicate absorption.

The wavelength coverage of the present observations is quite limited. We can extend the SED by considering the IRAC photometry obtained by GOODS at 3.6, 4.5, 5.8, and 8 μm, as well as the 16 μm photometry of Teplitz et al. (2006, in prep.). This extended spectral energy distribution (SED) shows that Source 2, at $z = 1.09$, appears indeed to be a typical, starburst-dominated LIRG as predicted by its other properties (see Figure 3). A clear emission peak is seen in the IRAC photometry, corresponding to the $\sim$ 1.6 μm opacity "bump" that is commonly observed in strong starbursts.

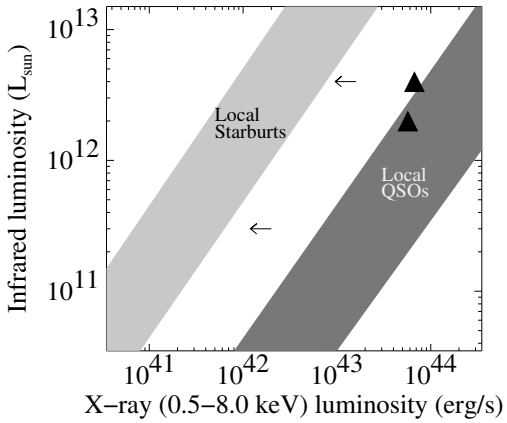

Figure 4. The X-ray luminosity vs. infrared luminosity plane for the target sources. The upper triangle indicates Source 1, the lower triangle Source 2-x, the top arrow indicates the upper limit for Source 1-BzK and the lower arrow indicates the upper limit for Source 2. Typical allowed values for local objects are indicated by shaded regions.

Source 1 at $z = 2.69$, on the other hand, does not show this "bump." In fact, its SED appears relatively featureless at all wavelengths shortward of 6.2 μm, extending into the NIR and optical. This featureless SED is consistent with the expectation for an X-ray source at high redshift. Source 1, therefore, is likely to be a composite object containing an AGN which dominates the emission in the near-IR, swamping the 1.6 μm bump, together with significant ongoing star formation which is responsible for the PAH emission. Source 1-BzK has a MIR SED similar to that of Source 1, lacking a prominent 1.6 μm bump.

The SED and MIR spectrum of Source 1 is a much better match to UGC 5101 (Armus et al. 2004). With UGC 5101 as a template, we can use its luminosity scaled to $z = 2.69$ to estimate the bolometric luminosity of Source 1 to be 4×10^{12} L$_\odot$. UGC 5101 has line ratios consistent with an AGN which contributes less than 10% of the bolometric luminosity, but deep silicate absorption leaves open the possibility of a larger contribution (Armus et al. 2004). Even a weak (10% of L_{bol}) AGN may produce enough hot dust emission in the NIR to hide the 1.6 μm bump. If we attribute all of the flux at restframe 5 μm to an AGN, and scale a representative AGN template (05189-2524 Armus et al. 2006) to that flux, we find a contribution of 1.6×10^{12} L$_\odot$ from the AGN to L$_{\rm Bol}$.

The ratio of L_X/L_{IR} in Source 1 is indeed consistent with significant AGN contribution (see Figure 4). Similarly, Source 1-BzK lies between the ratios typical of AGN- and starburst-dominated submillimeter galaxies (Alexander et al. 2005), while the detection limit for Source 2 constrains it to be closer to the locus of starburst galaxies. Source 2-x may be consistent with the ratio expected for an AGN-dominated SMG if it is at the adopted redshift.

4.1. Comparison with Other Surveys

The largest samples of IRS spectra of high-z galaxies were selected either using optical-to-MIR color properties. Houck et al. (2005) selected objects based on

very faint ($I_{AB} > 25$) optical magnitudes and detectable (≥ 0.8 mJy) 24 μm flux densities. Yan et al. (2005) used a less severe $R - 24$ selection function and also included the requirement of blue 8 to 24 μm color.

The sources in the present sample are much brighter in the optical, and much bluer, than the Houck et al. sources. This difference is not surprising given the rarity of the latter sources (33 in 8 square degrees). The $z > 2$ sources in the present sample meet the Yan et al. selection, but the lower redshift sources are bluer in $R - 24$. The Houck et al. and Yan et al. samples are not comprised exclusively of starbursts. Both surveys found substantial numbers of objects with spectra showing little PAH emission, likely indicating AGN-dominated sources. These objects are brighter than those in the current data by a factor of $\sim 5 - 7$, suggesting bolometric luminosities in excess of 10^{13} $L_\odot$.

Other recent surveys have used IRAC photometry to detect the 1.6 μm bump. As discussed above, Source 1 at $z = 2.69$ provides a striking example of a source that would be excluded by a "bump" survey but nonetheless has significant amounts of star formation contributing to its bolometric luminosity. Sources of this kind may be an important contribution to the global star formation density. It is difficult to estimate, however, based on current data how many such sources will be missed in IRAC surveys. This uncertainty demonstrates the need for wider use of deep MIR spectroscopy of high redshift sources.

Acknowledgments. This work is based in part on observations made with the *Spitzer Space Telescope*, which is operated by the Jet Propulsion Laboratory, California Institute of Technology under NASA contract 1407. Support for this work was provided by NASA through an award issued by JPL/Caltech.

References

Alexander, D. M., Bauer, F. E., Chapman, S. C., Smail, I., Blain, A. W., Brandt, W. N., & Ivison, R. J. 2005, ApJ, 632, 736
Armus, L., et al. 2004, ApJS, 154, 178
Armus, L., et al. 2006, ApJ, in press
Bell, E. F., et al. 2005, ApJ, 625, 23
Brand, K. et al. 2006, in press; astro-ph/0602198
Bushouse, H. A., et al. 2002, ApJS, 138, 1
Chary, R. & Elbaz, D. 2001, ApJ, 556, 562
Chary, R., et al. 2004, ApJS, 154, 80
Daddi, E., et al. 2005, ApJ, 631, L13
Houck, J. R., et al. 2004, ApJS, 154, 18
Houck, J. R., et al. 2005, ApJ, 622, L105
Lagache, G., et al. 2004, ApJS, 154, 112
Lutz, D., Valiante, E., Sturm, E., Genzel, R., Tacconi, L. J., Lehnert, M. D., Sternberg, A., & Baker, A. J. 2005, ApJ, 625, L83
Marleau, F. R., et al. 2004, ApJS, 154, 66
Papovich, C., et al. 2004, ApJS, 154, 70
Pérez-González, P. G., et al. 2005, ApJ, 630, 82
Ptak, A., Heckman, T., Levenson, N. A., Weaver, K., & Strickland, D. 2003, ApJ, 592, 782
Soifer, B. T., Sanders, D. B., Madore, B. F., Neugebauer, G., Danielson, G. E., Elias, J. H., Lonsdale, C. J., & Rice, W. L. 1987, ApJ, 320, 238
Vignati, P., et al. 1999, A&A, 349, L57
Yan, L., et al. 2005, ApJ, 628, 604